Calcium Binding to the Regulatory N-Domain of Skeletal Muscle Troponin C Occurs in a Stepwise Manner†

Monica X. Li, Stéphane M. Gagné, Sakae Tsuda, Cyril M. Kay, Lawrence B. Smillie, and Brian D. Sykes*

MRC Group in Protein Structure and Function, Department of Biochemistry, University of Alberta, Edmonton, Alberta, Canada T6G 2H7

Received December 20, 1994; Revised Manuscript Received April 20, 1995®

ABSTRACT: Ca^{2+} binding to a recombinant regulatory N-domain (residues 1−90) of chicken troponin C (NTnC) has been investigated with the use of heteronuclear multidimensional NMR spectroscopy. The protein has been cloned in pET3a vector and expressed in minimal media in *Escherichia coli* to allow uniform ^{15}N and ^{13}C labeling. The NMR spectra have been resolved and completely assigned [Gagné et al. (1994) *Protein Sci. 3*, 1961−1974]. Ca^{2+} titration monitored by 2D {^1H, ^{15}N}-HMQC NMR spectral changes revealed that Ca^{2+} binding to sites I and II of NTnC is a stepwise process and that chemical shift changes occur throughout the N-domain upon the binding of each Ca^{2+}. The Ca^{2+} dissociation constants for the binding of the first and second Ca^{2+} were determined to be 0.8 $\mu M \leq K_{d1} \leq 3$ μM and 5 $\mu M \leq K_{d2} \leq 23$ μM, respectively. This mechanism is believed to represent that of the N-domain in intact TnC since we have shown earlier that the properties of the N-domain (1−90) were identical to those of the N-domain in intact TnC [Li et al. (1994) *Biochemistry 33*, 917−925]. In contrast, however, our previous Ca^{2+} fluorescence and far-UV CD studies on F29W NTnC and F29W TnC indicated cooperative Ca^{2+} binding to sites I/II and no detectable differences in their affinities. To rationalize these observations, a direct comparison was made of the Ca^{2+} titration of NTnC and F29W NTnC as monitored by far-UV CD spectroscopy. Unlike F29W NTnC, NTnC gave a biphasic curve with binding constants in reasonable agreement with the NMR data. Although the far-UV CD spectra of NTnC and the F29W NTnC domain were the same in the absence of Ca^{2+}, the Ca^{2+}-induced negative ellipticity increase for NTnC is significantly smaller than for F29W NTnC. These observations indicate that the F29W mutation has perturbed the Ca^{2+} binding properties of the N-domain and its CD spectroscopic properties in the Ca^{2+}-saturated state.

The crystal structure of avian skeletal troponin C (TnC)[1] has been solved and the molecule shown to be dumbbell-shaped with two globular domains connected by an extended α-helix (Herzberg & James, 1988; Satyshur et al., 1988). The N-domain contains a pair of divalent metal binding sites (I/II), unoccupied in the X-ray structure, and believed to be Ca^{2+}-specific with association constants in the 10^5-10^6 M^{-1} range. Another pair of divalent metal binding sites (III/IV) are located in the C-domain. These sites are loaded with Ca^{2+} in the X-ray structure and have a higher affinity for Ca^{2+} ($K_a \approx 10^7$ M^{-1}) and also bind Mg^{2+} ($K_a \approx 10^3$ M^{-1}) [for reviews, see Leavis and Gergely (1984), Zot and Potter (1987c), and Grabarek et al. (1992)]. Each site consists of the helix−loop−helix motif typical of this class of proteins [for a review, see Strynadka and James (1989)]. The C-terminal domain, whose sites III/IV are believed to be always saturated with Ca^{2+} or Mg^{2+} *in vivo*, is believed to play a structural role, while the N-terminal domain is considered to play the regulatory role.

The regulatory function is associated with the conformational change in TnC induced by Ca^{2+} binding to sites I/II in the N-domain, the resultant signal transmission to the other members of the thin filaments (troponin I, troponin T, tropomyosin, and actin), the modified interaction between the thick and thin filaments, and, ultimately, muscle contraction [for reviews, see Leavis and Gergely (1984), Zot and Potter (1987c), and Grabarek et al. (1992)]. The nature of the Ca^{2+}-triggered conformational transition in TnC and its signal transmission mechanisms are not yet clear, although a model has been proposed for the Ca^{2+}-induced structural transition of the N-domain (Herzberg et al., 1986). This conformational change would involve a rearrangement of secondary structural elements such that helices B and C move away as a unit relative to N, A, and D helices to expose a hydrophobic patch on the surface of the molecule. While several studies have been designed to test the validity of the model and have provided support for its general features [reviewed by Grabarek et al. (1992); Pearlstone et al. (1992a); see, however, Pearlstone et al. (1992b)], the most direct support has recently come from NMR determination of TnC's N-domain secondary structure (Gagné et al., 1994). Although these NMR solution studies provide vital information on the end states (apo and $2Ca^{2+}$), it is important to understand the sequential processes involved in the binding of Ca^{2+} to sites I/II of this regulatory domain.

Several groups have examined Ca^{2+} and/or Mg^{2+} binding to TnC or its isolated fragments by direct binding measure-

† This study was supported by the Medical Research Council of Canada. M.X.L. was supported by a postdoctoral fellowship from the Alberta Heritage Foundation for Medical Research and S.M.G. by a FCAR fellowship from the Province of Québec.

® Abstract published in *Advance ACS Abstracts,* June 15, 1995.

[1] Abbreviations: TnC, troponin C; NTnC, N-domain (residues 1−90) of recombinant chicken troponin C; NMR, nuclear magnetic resonance; HMQC, heteronuclear multiple-quantum coherence; CD, circular dichroism.

0006-2960/95/0434-8330$09.00/0

ments (Potter & Gergely, 1975; Iida, 1988; Fujimori et al., 1990; da Silva et al., 1993), by spectroscopic techniques such as fluorescence and CD (Leavis et al., 1978; Johnson et al., 1978, 1979; Hincke et al., 1978; Potter et al., 1981; Grabarek et al., 1983, 1990; Griffiths et al., 1984; Zot et al., 1986; Zot & Potter, 1987a,b, 1989; Güth & Potter, 1987; Ellis et al., 1988; Golosinska et al.; 1991; Pearlstone et al.; 1992a,b; Li et al., 1994; Chandra et al., 1994), by microcalorimetry (Brzeska et al., 1983; Tsalkova & Privalov, 1985; Imaizumi et al., 1987, 1990; Imaizumi & Tanokura, 1990), and by NMR (Levine et al., 1977; Seamon et al., 1977; Leavis et al., 1980; Evans et al., 1980; Drabikowski et al., 1985; Drakenberg et al., 1987; Tsuda et al., 1988, 1990). Most of the fluorescence measurements have involved introducing spectral probes either by covalently linking aromatic groups to specific amino acid residues or by site-specific mutagenesis, modifications which to some degree may perturb the native properties of the protein. While CD monitors the global conformational changes in proteins, NMR can report information that pertains to individual atoms throughout the sequence. However, most of the ^{1}H-NMR work has been hampered since only a few resonances could be assigned due to the severe overlap in the ^{1}H-NMR spectra of a molecule with the high α-helical content and size of TnC. Recently, triple resonance multidimensional NMR in combination with ^{13}C/^{15}N double labeling of proteins has greatly simplified the assignment of NMR spectra by resolving most of the overlapping signals. These techniques have permitted the determination of structures in solution for proteins the size of TnC, such as calmodulin (Ikura et al., 1992). Similar approaches have also been applied to the study of Ca^{2+} binding to cardiac TnC (Krudy et al., 1992), which differs from skeletal TnC in having one nonfunctional Ca^{2+} binding site in the N-domain.

We have shown recently that isolated N-domain fragment 1−90 of TnC (NTnC) appears to have identical properties to that of the N-domain of the intact protein (Li et al., 1994). By using uniformly ^{15}N- and ^{13}C-labeled NTnC and using 3D triple resonance techniques, we were able to complete the backbone resonance assignments for the apo (^{1}H, ^{15}N) and Ca^{2+} (^{1}H, ^{15}N, and ^{13}C) states of NTnC (Gagné et al., 1994). These assigned resonances are used in this paper to monitor a detailed Ca^{2+} titration using 2D {^{1}H, ^{15}N}-HMQC NMR spectra and to focus on the Ca^{2+} binding mechanism. The HMQC titration results indicate that Ca^{2+} binding to this important regulatory domain is a stepwise binding process with the Ca^{2+} affinity to one site approximately 8−10-fold stronger than to the other.

Previously, we have shown that a F29W mutant of chicken recombinant TnC serves as a useful and specific fluorescence probe for the Ca^{2+}-induced structural transition of the N-domain in intact TnC (Pearlstone et al., 1992a). On the basis of far-UV CD studies, it seemed that substitution of Phe29 by Trp had minimal effects on the global fold and on the Ca^{2+} binding properties of the intact molecule. Calcium titration fluorescence and far-UV CD measurements of mutants F29W NTnC and intact F29W TnC indicated cooperative Ca^{2+} binding to sites I/II and no detectable differences in their affinities (Li et al., 1994). In order to rationalize these differences with the present NMR data, a direct comparison was made of the Ca^{2+} titration of NTnC and F29W NTnC as monitored by far-UV CD. Unlike F29W NTnC, the wild-type NTnC gave a biphasic curve with binding constants in reasonable agreement with the NMR data. Significant differences in the far-UV CD spectra of the two N-domains in the $2Ca^{2+}$ state were also observed. The observations indicate that the F29W mutation has perturbed the Ca^{2+} binding properties and its CD spectroscopic propeties in the Ca^{2+}-saturated state.

EXPERIMENTAL PROCEDURES

The engineering of expression vectors, expression in *Escherichia coli*, and purification of wild-type NTnC and F29W NTnC were as described (Li et al., 1994; Gagné et al., 1994). Far-UV CD spectral measurements, preparation of buffers and stock protein solutions, calcium titrations, calculations of free [Ca^{2+}], data analyses, protein concentration determinations, and curve-fitting of the Ca^{2+} titration data were as described previously (Golosinska et al., 1991; Pearlstone et al., 1992a).

NMR Sample Preparation. The expression and purification of [^{15}N]-NTnC were as described in Gagné et al. (1994). To obtain metal-free [^{15}N]-NTnC, 10 mg of protein was dissolved in 0.5 mL of 25 mM NH_4HCO_3 and 100 mM EDTA. This was then applied to a 160-mL (1.5 × 90 cm) G-25 gel filtration column equilibrated and eluted with 25 mM NH_4HCO_3 and monitored at $\lambda = 254$ nm. The metal-free NTnC was eluted first, well resolved from EDTA and metal ions. The pooled protein fractions were lyophilized, redissolved in water, and lyophilized again for efficient removal of NH_4HCO_3. Milli-Q deionized water and plastic vessels were used in all steps. The NMR sample was prepared by dissolving 10 mg of metal-free [^{15}N]-NTnC in 0.5 mL of 100 mM KCl in 90% H_2O/10% D_2O in an Eppendorf tube. To the sample were added 5 μL of 100 mM DSS in D_2O and 5 μL of 1.3% NaN_3 in D_2O. Following adjustment to pH 6.6 with HCl and/or NaOH, 0.5 mL was transferred to the NMR tube. The concentration of protein was determined to be 1.5 mM by amino acid analyses in triplicate. All buffer and reagent solutions used in this study were treated with Chelex 100 before use to remove metal contaminants.

Calcium Titration of [^{15}N]-NTnC Monitored by {^{1}H, ^{15}N}-HMQC Spectra. A stock solution of 50 mM $CaCl_2$ in 90% H_2O/10% D_2O was prepared from a standarized 100 mM $CaCl_2$ solution in water (Golosinska et al., 1991). With a 10 μL Hamilton syringe, aliquots of 5 μL of stock $CaCl_2$ were added to the NMR tube for each titration point and mixed thoroughly. The total volume increase was 45 μL, and the change in protein concentration due to dilution was not taken into account for data analyses. The change in pH from $CaCl_2$ addition was negligible.

NMR Spectroscopy. ^{1}H/^{15}N heteronuclear multiple quantum coherence spectra (HMQC; Bax et al., 1983) were recorded on a Varian VXR 500 NMR spectrometer at 30 °C and acquired with ^{15}N decoupling during the acquisition period (WALTZ-16; Shaka et al., 1983). Each spectrum was collected with 704 complex data points in the t_2 dimension and 320 complex data points in t_1; 32 transients per FID were recorded. The ^{1}H and ^{15}N sweep widths were 7000 and 3000 Hz, respectively. Suppression of the water resonance was achieved by presaturation (2.0−2.5 s). Total acquisition time for each spectrum was 9 h. Data were zero-filled in both dimensions to generate a final 2048 × 1024 points spectrum. Processing of the data sets was accomplished on a SUN IPC workstation using the VNMR software package (VNMR 4.1A, Varian, Palo Alto, CA).

RESULTS

HMQC Spectra. A series of {^{1}H, ^{15}N}-HMQC NMR spectra depicting the amide region from the Ca^{2+} titration of [^{15}N]-NTnC is shown in Figure 1. Expanded regions (7.1−9.1 ppm for NH and 115−126 ppm for ^{15}N) are shown in Figure 2. These spectra are well resolved, demonstrating the feasibility of using heteronuclear multidimensional NMR to follow individual amide NH resonance during Ca^{2+} titration. Both apo (panel A in Figures 1 and 2) and Ca^{2+}-saturated (panel J in Figures 1 and 2) spectra have been completely assigned to the corresponding residues in the protein (Gagné et al., 1994). The chemical shift values of backbone ^{15}N and NH groups for both apo and Ca^{2+}-saturated states are listed in Table 1. Residues listed as unassigned were not observed. The addition of Ca^{2+} to NTnC caused dramatic changes in the HMQC spectra as shown in Figures 1 and 2 and reflects the Ca^{2+}-induced conformational changes in the molecule. The NMR spectral changes can occur in fast, intermediate, and/or slow exchange limit on the NMR time scale depending on the size of the Ca^{2+}-induced resonance shift. It is believed that Ca^{2+} binding to sites I/II of TnC is diffusion-controlled with an on rate (k_{on}) of $\sim 10^8$ M^{-1} s^{-1} and k_{off} ranges from 10^2 to 10^3 s^{-1} [for a review, see Potter and Johnson (1982)]. Hence, Ca^{2+} binding to the N-domain of TnC would occur with a τ_{ex} of 0.01−0.001 s ($\tau_{ex} = 1/k_{off}$). Fast exchange conditions exist for the resonances with $(\tau_{ex}\Delta)^2 \ll 1$, and slow exchange conditions exist for the resonances with $(\tau_{ex}\Delta)^2 \gg 1$, where $\Delta = |\delta_{Ca} - \delta_{apo}|$. For instance, for a resonance with a 1 ppm shift in the ^{1}H dimension on a 500 MHz spectrometer and with $\tau_{ex} = 0.005$ s, $(\tau_{ex}\Delta)^2 = [(2\pi)(500)(0.005)]^2 = 246 \gg 1$; slow exchange behavior would be observed for this peak. On the other hand, for a resonance with a 0.01 ppm shift, $(\tau_{ex}\Delta)^2 = [(2\pi)(5)(0.005)]^2 = 0.025 \ll 1$, its spectral changes would be in the fast exchange regime. Some resonances can fall between the slow and fast exchange limits, i.e., intermediate exchange with $(\tau_{ex}\Delta)^2 \approx 1$, and are characterized by line broadening during Ca^{2+} titration. In the present HMQC NMR titration, the majority of the cross-peaks stayed sharp, gradually shifted in the ^{1}H and/or ^{15}N dimensions during titration, and were presented at each point of the titration. These peaks correspond to those residues in the fast exchange limit on the NMR time scale, and they can be followed to monitor the Ca^{2+} titration, among which G69, G33, and G43 are typical examples as marked in Figure 1. All the resonances listed in the Figure 4 legend (see Figures 1 and 2 for labels) also belong to this category. Some resonances, such as R11, F13, S15, E17, Q51, N52, K55, and A90, show very small chemical shift changes (see Table 1; R11 and A90 are marked in Figures 1 and 2 as examples) as Ca^{2+} is added, and they are usually located in the regions which undergo the least conformational changes during Ca^{2+} titration. Although most of the residues in NTnC undergo fast exchange with Ca^{2+}, slow exchange was observed for a number of residues, such as I37 and I73. As shown in Figures 1 and 2, separate resonances for I37 and I73 were observed in the apo spectrum and Ca^{2+}-saturated spectrum accompanied with very big chemical shift changes and disappearence of peaks during titration. As shown in Table 1 for I37, the NH chemical shift changed from 8.31 to 9.61 ppm and the ^{15}N chemical shift changed from 111.9 to 125.9 ppm; for I73, the changes were from 8.87 to 9.19 ppm and from 118.3 to 126.5 ppm, respectively. A31, G34, G35, S38, T39, E41, L42, I62, V65, E67, and G71 as shown in Figure 1A,J and Figure 2A,J also fall into this category (see Table 1 for ppm values). These residues are located in the centers of the Ca^{2+} binding loops I and II and are most affected by the Ca^{2+} binding. The typical intermediate exchange is exemplified by K23, G50, and V80, as observed in Figures 1 and 2. Their resonances start as sharp peaks and then broaden with the decrease of peak intensities and sharpening up again as the $[Ca]_{total}/[NTnC]_{total}$ ratio is increased. The two most downfield-shifted resonances in the apo state are from Gly35 and Gly71 as marked in Figure 1, indicating that these two glycines in NTnC are involved in hydrogen bonds even in the absence of Ca^{2+}. This is consistent with the NMR study of cardiac TnC (Krudy et al., 1992). The hydrogen bonds become stronger in the Ca^{2+}-bound state as suggested by the shifts to lower fields as shown in Figure 1 and Table 1.

The absolute chemical shift change differences for NH and ^{15}N between apo and $1Ca^{2+}$ states and between apo and $2Ca^{2+}$ states are plotted in Figure 3. The chemical shift changes occur throughout the sequence when the $[Ca]_{total}/[NTnC]_{total}$ ratio goes from 0 to 1, indicating 1 equiv of Ca^{2+} is sufficient to induce a global structural change in NTnC. When a second equivalent of Ca^{2+} is added, further chemical shift changes are also distributed throughout the sequence. This demonstrates that conformational changes induced by Ca^{2+} binding to either site of NTnC are propagated globally. As expected, the most perturbed amides are those located in the calcium binding loops as shown in Figure 3A,C. It seems that loop II is more affected than loop I in binding the first equivalent of Ca^{2+} as shown in Figure 3B,D, implying that site II in NTnC binds Ca^{2+} first. However, there are less data bars in Figure 3B,D because less cross-peaks are observed (Figures 1D and 2D) when the $[Ca]_{total}/[NTnC]_{total}$ ratio is 1. Therefore, this observation must be intepreted with caution, and this work is inconclusive in terms of the Ca^{2+} binding order to sites I/II of NTnC.

Ca^{2+} Binding Constants from HMQC Titration. The resonances of residues which showed NH and/or ^{15}N chemical shift changes in the intermediate to fast exchange limit during the Ca^{2+} titration were followed, and these changes were normalized and plotted as a function of the $[Ca]_{total}/[NTnC]_{total}$ ratio (see Figure 4). For purposes of clarity, the plots are shown in groups of 10 in each panel (see following for the fitted curves in the plots) and the data points are only shown for 2 residues in each panel. The Ca^{2+} binding equilibria for a two-site protein such as NTnC are shown in Figure 5. The plots in Figure 4 reflect the species distribution from the equilibria shown in Figure 5. For a more detailed description of the use of distribution plots to extract binding parameters from NMR data, see the Appendix in Williams et al. (1987). The computer program crvfitS (R. Boyko and B. D. Sykes, University of Alberta) was used for the fitting. The fitting of each set of titration data involves four variables: α, K_{d1}, K_{d2}, and S. S is defined as the fraction of total chemical shift observed after addition of 1 equiv of Ca^{2+} ($0 \le S \le 1$). Starting from initial estimates of the microscopic dissociation constants K_{d1} and K_{d2}, and with the cooperativity $\alpha = 1$, an S value was chosen for each residue and varied to obtain the lowest standard deviation (χ) between the calculated curve and observed data points. The χ value was then calculated as a function of K_{d1} and K_{d2}, where K_{d1} and K_{d2} were varied over the range: $0.1\ \mu M \le K_{d1} \le 8\ \mu M$ and $5\ \mu M \le K_{d2} \le 80\ \mu M$. This

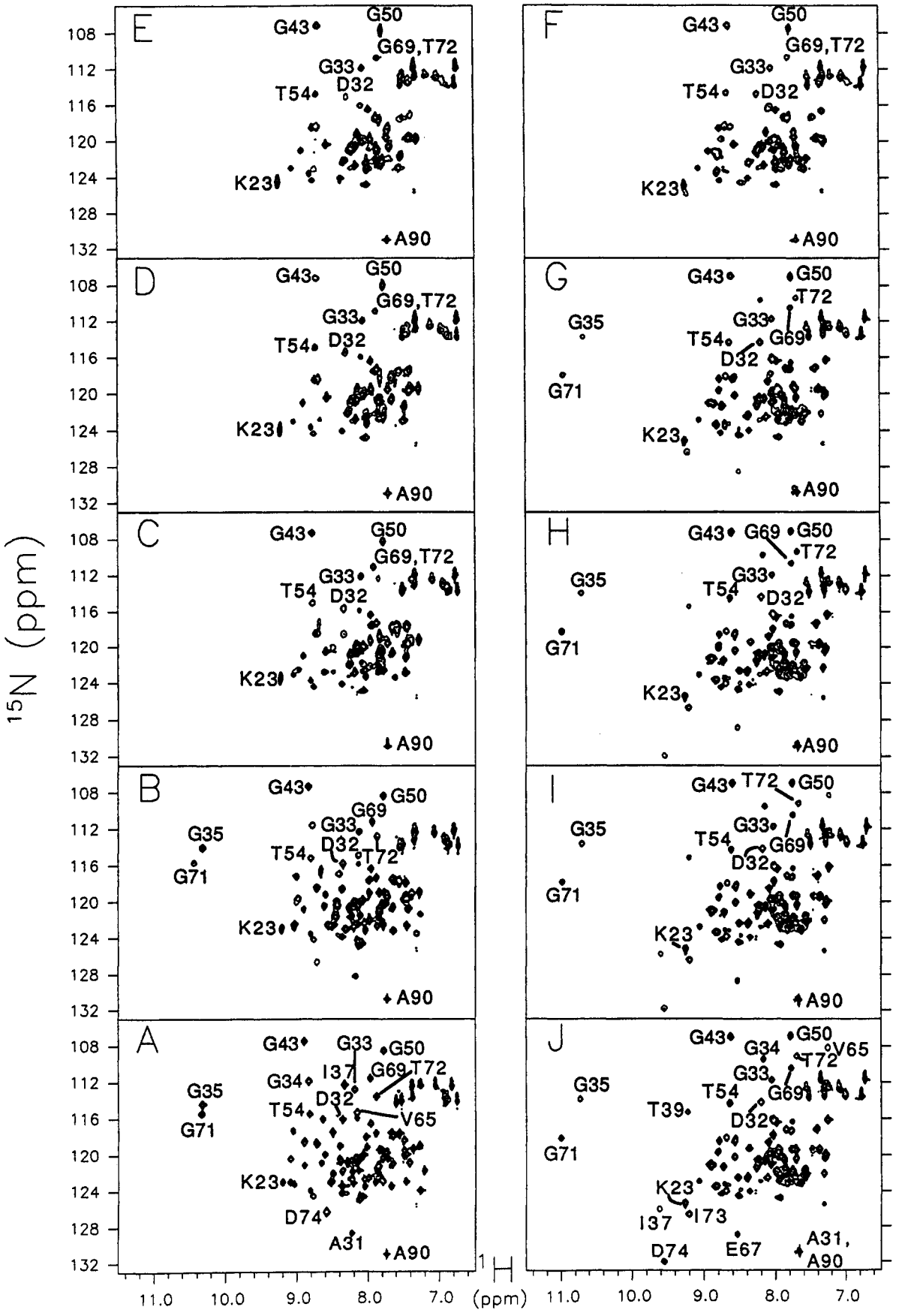

FIGURE 1: Amide regions of the {^{1}H,^{15}N}-HMQC NMR spectra of 1.5 mM uniformly ^{15}N-labeled NTnC, shown at the following $[Ca]_{total}/[NTnC]_{total}$ ratios: (A) 0.00, (B) 0.33, (C) 0.67, (D) 1.00, (E) 1.33, (F) 1.67, (G) 2.00, (H) 2.33, (I) 2.67, (J) 3.00. Resonances for some residues are as marked on the spectra. Conditions are described under Experimental Procedures.

process was then iterated to determine the values for K_{d1}, K_{d2}, and S which gave the lowest χ. In principal, all data sets can be fitted together, but 6 groups of 10 residues were fitted separately as shown in Figure 4. A typical contour

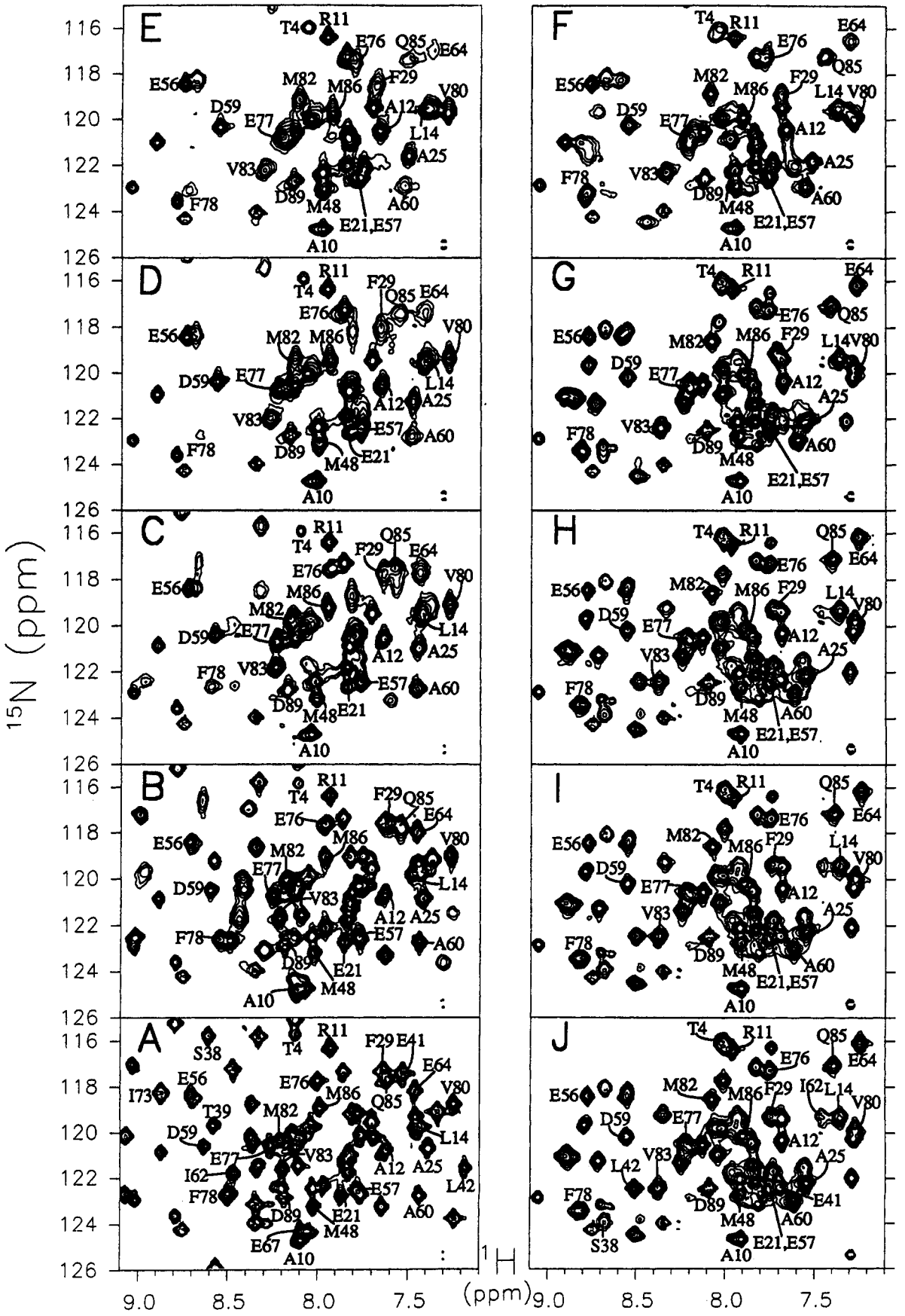

FIGURE 2: Expanded regions of Figure 1 with the following $[Ca]_{total}/[NTnC]_{total}$ ratios: (A) 0.00, (B) 0.33, (C) 0.67, (D) 1.00, (E) 1.33, (F) 1.67, (G) 2.00, (H) 2.33, (I) 2.67, (J) 3.00. Resonances for some residues are as marked on the spectra. Conditions are described under Experimental Procedures.

plot of χ versus K_{d1} and K_{d2} is shown in Figure 6 for the residues shown in Figure 4B [see Campbell et al. (1991)]. The contours with the lowest χ values from each of the six fits (Figure 4A–F) enclose similar regions. The best-fit

Table 1: ^{1}HN and ^{15}N Chemical Shifts for the Apo and 2Ca^{2+} N-Domain of Chicken Recombinant Troponin C at pH 6.6 and 30 °C

residue	^{1}H(apo)	^{1}H(2Ca^{2+})	^{15}N(apo)	^{15}N(2Ca^{2+})	residue	^{1}H(apo)	^{1}H(2Ca^{2+})	^{15}N(apo)	^{15}N(2Ca^{2+})
A1					M46	8.35	8.01	118.7	117.7
S2					R47	8.12	8.22	120.2	120.5
M3					M48	8.01	7.94	123.2	122.8
T4	8.12	8.01	115.7	116.1	L49	7.33	7.19	119.0	
D5	8.34	8.69	121.6	123.0	G50	7.74	7.75	108.2	106.9
Q6	8.29	8.87	121.5	120.9	Q51	8.03	7.95	119.6	119.4
Q7	8.18	7.83	122.3	123.0	N52	8.69	8.66	118.5	118.0
A8	8.05	8.50	124.3	124.4	P53				
E9	8.12	8.13	120.6	120.5	T54	8.79	8.60	115.1	114.3
A10	8.10	7.92	124.8	124.5	K55	8.78	8.79	123.7	123.3
R11	7.93	7.96	116.4	116.5	E56	8.75	8.80	118.3	118.3
A12	7.61	7.69	120.8	120.4	E57	7.79	7.77	122.4	122.6
F13	7.69	7.68	119.4	119.4	L58	8.50	7.96	122.6	121.6
L14	7.42	7.37	119.8	119.4	D59	8.63	8.54	120.6	120.1
S15	7.86	7.83	117.3	117.2	A60	7.42	7.63	122.7	123.0
E16	9.00	9.05	122.9	122.7	I61	7.94	7.57	122.3	121.5
E17	8.87	8.89	120.8	120.9	I62	8.45	7.46	121.8	119.3
M18	7.75	7.73	122.7	121.6	E63	7.76	8.35	119.1	119.1
I19	8.09	8.24	120.7	121.2	E64	7.46	7.27	118.1	116.2
A20	7.83	7.84	121.1	122.2	V65	8.11	7.26	115.0	108.3
E21	7.85	7.77	122.8	122.2	D66	8.34		123.1	
F22	9.04	8.72	122.7	121.2	E67	8.07	8.53	124.3	128.7
K23	9.17	9.24	122.7	125.1	D68	8.45	8.01	117.2	116.2
A24	7.84	7.57	121.7	122.2	G69	7.93	7.75	111.3	110.4
A25	7.38	7.57	120.8	122.0	S70	9.05	8.54	120.1	118.2
F26	8.35	8.88	120.3	121.2	G71	10.28	10.97	115.1	118.0
D27	9.02	8.57	116.8	118.6	T72	7.88	7.68	113.3	109.3
M28	7.45	7.30	119.3	120.3	I73	8.87	9.19	118.3	126.5
F29	7.64	7.78	117.3	119.4	D74	8.57	9.53	126.0	131.9
D30	7.24	8.08	123.7	119.7	F75	8.36	8.79	120.1	119.7
A31	8.15	7.68	128.4	130.4	E76	7.96	7.77	117.8	117.3
D32	8.33	8.19	115.8	114.3	E77	8.27	8.19	120.5	120.7
G33	8.13	8.02	112.6	111.8	F78	8.46	8.83	122.7	123.4
G34	8.78	8.14	111.6	109.6	L79	8.11	8.02	120.2	119.8
G35	10.28	10.69	114.0	113.8	V80	7.25	7.29	118.8	120.3
D36	7.81	7.75	119.1	116.2	M81	7.75	7.85	119.9	121.5
I37	8.31	9.61	111.9	125.9	M82	8.18	8.07	120.3	118.6
S38	8.58	8.70	115.8	124.0	V83	8.19	8.38	121.5	122.3
T39	8.58	9.22	119.6	115.1	R84	7.68	8.06	120.2	120.8
K40	8.10	7.84	121.4	122.7	Q85	7.59	7.40	117.7	117.2
E41	7.53	7.70	117.3	122.3	M86	7.93	7.92	118.8	120.1
L42	7.19	8.52	121.4	122.4	K87	7.79	7.86	120.9	120.4
G43	8.84	8.58	107.1	107.1	E88	8.10	7.91	122.3	121.9
T44	7.45	7.94	119.8	119.7	D89	8.20	8.08	122.8	122.3
V45	7.63	7.30	123.2	122.0	A90	7.70	7.65	130.8	130.7

region (lowest χ values) is defined by 0.8 μM $\leq K_{d1} \leq$ 3 μM and 5 μM $\leq K_{d2} \leq$ 23 μM. Higher χ values were obtained when $0 < \alpha < 1$, which indicates positive cooperativity, or $\alpha > 1$, which indicates negative cooperativity. The rather large uncertainties of K_{d1} and K_{d2} were not unexpected because a degree of uncertainty is involved in the determined binding constants when the dissociation binding constants are less than the concentrations of the protein required for NMR experiments (Williams et al., 1985). These results quantitatively demonstrate the stepwise binding of 2 mol of Ca^{2+} to sites I and II of skeletal muscle TnC. The derived macroscopic dissociation constants based on the defined equations [see Figure 5 and Williams et al. (1985)] are 0.69 μM $\leq K_{D1} \leq$ 2.65 μM and 5.8 μM $\leq K_{D2} \leq$ 26 μM. These K_D values fall in the range of those previously reported for the low-affinity sites of TnC [for a review, see Leavis and Gergely (1984)].

Ca^{2+} Binding Curves from HMQC Titration. The resultant fitted curves are shown in Figure 4 for 0.8 μM $\leq K_{d1} \leq$ 3 μM, 5 μM $\leq K_{d2} \leq$ 23 μM, and $\alpha = 1$. Each curve is characterized by a specific S value defined as the fraction of the total chemical shift observed after addition of 1 equiv of Ca^{2+} (see above). Values of S (generally $0 \leq S \leq 1$) decrease from left to right in each panel. All the curves can be generally summarized into three types as indicated in Figure 4A. Type I indicates that the structural transition is completed after the addition of only 1 equiv of Ca^{2+}, type II shows the transition is equally sensitive to the filling of each of the two sites by Ca^{2+}, and type III shows the transition remains unchanged when the first equivalent of Ca^{2+} is added and increases upon addition of the second equivalent. Values of S are ~1 for type I, ~0.5 for type II, and ~0 for type III curves. Residues which give curves between type I and type II have $0.5 \leq S \leq 1$ and are more sensitive to the the first Ca^{2+} filling than to the second. Residues which give curves between type II and type III have $0 \leq S \leq 0.5$ and are more sensitive to the second than to the first. The data clearly show the sequential nature of Ca^{2+} binding to sites I/II of TnC. If site I and site II bound Ca^{2+} ions with high positive cooperativity or bound Ca^{2+} ions independently but with equal affinities, only type II curves would be observed. The residues which give type I curves are distributed all along the sequence (for instance, T4, L14, G33, R47, D59, S70, E77, V80) as are type II (e.g., A10, K23, E64, T72, V83, M86) and type III (e.g., M18, A24, D32, M48, G50, A60, F78, E88, D89) residues. For each group of curves shown in each panel, the corresponding residues are randomly located along the sequence. This behavior also indicates that

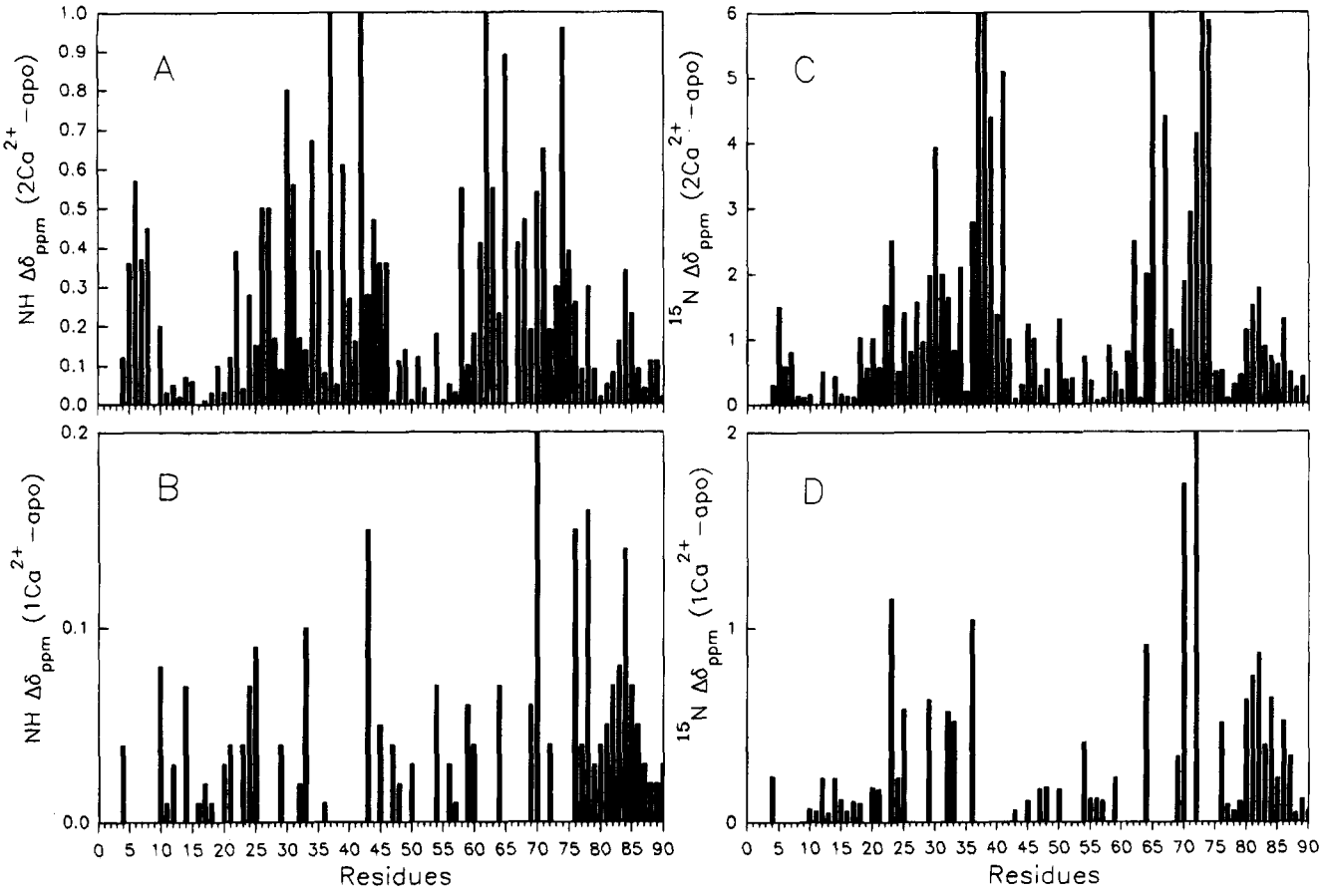

FIGURE 3: Plots of chemical shift changes (absolute values) for [^{15}N]-NTnC: (A) apo to 2Ca^{2+} state for NH; (B) apo to 1Ca^{2+} state for NH; (C) apo to 2 Ca^{2+} state for ^{15}N; (D) apo to 1Ca^{2+} state for ^{15}N.

although Ca^{2+} binding to NTnC is clearly a stepwise binding process, the binding order cannot be determined based on this work.

Far-UV CD Studies. The far-UV CD spectra of NTnC and F29W NTnC in the absence and presence of Ca^{2+} (pCa = 3) are shown in Figure 7. Two minima are observed for both proteins in both apo and Ca^{2+} states, one at 208 nm, the other at 221 nm. Spectral features in the apo states are seen to be virtually superimposable for NTnC and F29W NTnC, while obvious discrepancies are observed in the Ca^{2+}-loaded states. As observed from Figure 7, the ratio of two minima ($[\theta]_{208nm}$:$[\theta]_{221nm}$) in the Ca^{2+} state is ~1.2 for NTnC, whereas for F29W NTnC it is ~1. For NTnC, the negative ellipticity change at 221 nm from a pCa of 8 to the Ca^{2+} state (pCa of 3) is from 15 500 ± 500 to 17 600 ± 400 deg·cm^2·dmol^{-1} with a difference of 2100 deg·cm^2·dmol^{-1}; for F29W NTnC, this change was 3500 deg·cm^2·dmol^{-1} [15 400 ± 700 to 18 900 ± 600 deg·cm^2·dmol^{-1} (Li et al., 1994)]. The results suggest that the Ca^{2+}-evoked structural alteration for F29W NTnC and wild-type NTnC are not identical.

Titrations of the $[\theta]_{221nm}$ changes of NTnC and F29W NTnC as a function of pCa are shown in Figure 8. In contrast to the monophasic curve observed for F29W NTnC [$-\log K_D = 5.80 \pm 0.03$ (Li et al., 1994)], a biphasic curve was best-fitted to the averaged titration data of NTnC by attributing 20% of the total $[\theta]_{221nm}$ changes to the lower affinity site and 80% to the higher affinity site in the N-domain. The derived two binding constants for NTnC are $-\log K_{D1} = 5.51$ (±0.02) and $-\log K_{D2} = 4.29$ (±0.01), which are in reasonable agreement with the NMR data, 6.19 $\geq -\log K_{D1} \geq 5.58$ and $5.24 \geq -\log K_{D2} \geq 4.59$. The results reinforce the conclusion from the NMR studies that Ca^{2+} binding to the N-domain of TnC occurs in a stepwise fashion with one site about 8−10 times stronger than the other. The data also indicate that the substitution of Phe29 by Trp has perturbed the Ca^{2+} binding properties of the N-domain.

DISCUSSION

We have studied in detail the mechanism of Ca^{2+} binding to NTnC as monitored by {^{1}H, ^{15}N}-HMQC NMR spectra. This study was considered to be advantageous over previous ones for the following reasons. First, by using NTnC, which by all criteria examined have identical properties to the N-domain in the intact molecule (Li et al., 1994) and the same secondary structure as the apo N-domain in the crystallographic structure of intact TnC (Gagné et al., 1994), a high background of divalent metal ion-induced changes attributable to C-domain sites III/IV could be avoided. Although the TR$_1$C fragment (residues 9−84 of rabbit TnC) has been used to study Ca^{2+} binding to the low-affinity sites I/II (Leavis et al., 1978; Drakenberg et al., 1987), it was observed that the Ca^{2+}-induced structural transition of TR$_1$C is not fully representative of that occurring in the N-domain of intact TnC (Li et al., 1994). Differences were also observed between the NMR structure of this fragment in the apo state (Findley & Sykes, 1993; Findlay et al., 1994) and the corresponding region of the crystallographic structure and NMR structure of NTnC (Gagné et al., 1994; Gagné et al., in preparation). Second, by using 2D {^{1}H,^{15}N}-HMQC

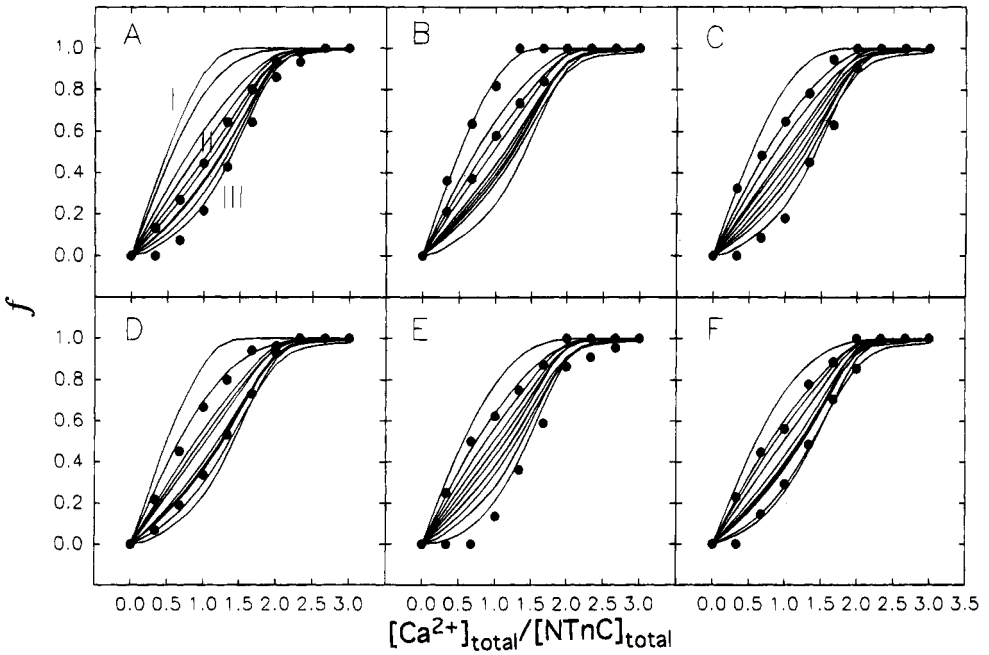

FIGURE 4: Calcium titration plots derived from Figures 1 and 2. f represents the normalized chemical shift change for different resonances, which was plotted vs $[Ca]_{total}/[NTnC]_{total}$. The curves are the best-fit lines through the titration data points (only shown for two resonances in each panel as indicated by boldface letters below). The curves (from left to right) in each panel correspond to the following resonances: (A) E76(^{15}N), E77(NH)/R47(NH), **K23(NH)**, M82(^{15}N), K23(^{15}N), T54(NH), F29(^{15}N), G69(NH), F78(^{15}N), **A60(NH)**; (B) **G33(^{15}N)**, L14(NH), **G43(NH)**, Q85(^{15}N), M86(^{15}N), E57(^{15}N), E21(^{15}N), D32(^{15}N), D89(^{15}N), A60(^{15}N); (C) D59(NH), **T4(^{15}N)**, E76(NH), A10-(NH), E64(^{15}N), V45(^{15}N), E56(NH), A24(^{15}N), E88(NH), **D32(NH)**; (D) S70(^{15}N), **S70(NH)**, F78(NH), A25(NH), T72(^{15}N), V45(NH), A20(^{15}N), **E64(NH)**, E88(^{15}N), M48(NH); (E) V80(NH), **M86(NH)**, A12(^{15}N), T54(^{15}N), V83(^{15}N), L79(^{15}N), D36(^{15}N), F29(NH), A24-(NH), **G50(^{15}N)**; (F) G33(NH), **M82(NH)**, D59(^{15}N), R84(NH), V80(^{15}N), A25(^{15}N), T4(NH), E41(^{15}N), **D89(NH)**, M18(^{15}N).

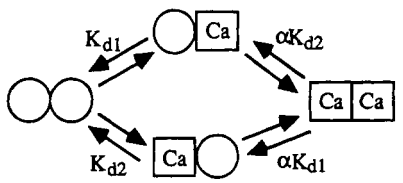

FIGURE 5: Ca^{2+} binding equilibria for a two-site protein molecule. K_{d1} and K_{d2} are the microscopic dissociation constants for the two sites. α is the degree of cooperativity ($0 < \alpha < 1$ for positive cooperativity, $\alpha = 1$ for no cooperativity, $\alpha > 1$ for negative cooperativity). K_{D1} and K_{D2} are the macroscopic dissociation constants. $K_{D1} = K_{d1}K_{d2}/(K_{d1} + K_{d2})$, $K_{D1}K_{D2} = \alpha K_{d1}K_{d2}$. P represents the apo form of a protein molecule, PCa a protein molecule with one Ca^{2+} ion bound to either site, and PCa_2 a protein molecule with both sites occupied.

NMR spectra changes to monitor Ca^{2+} binding, the problem of overlapping resonances from different residues as often encountered in ^{1}H-NMR has been overcome. In most of the ^{1}H-NMR studies of TnC and its fragments, only a few resonances could be assigned, and the interpretation based on the limited assignments could be misleading. For example, the gradual parallel increase in type II curves (see Figure 4A) when adding 2 equiv of Ca^{2+} suggests that binding of the two ions takes place in a positive cooperative manner or the two sites have equal affinity for Ca^{2+}. Thus, if only this type of residue was monitored, a false interpretation would be made. In the present work, resonances from residues throughout the sequence of the N-domain were followed in the titration, and they are highly informative probes of the Ca^{2+}-induced conformational changes in every region of the structure. Thus, the spectral changes monitored are a result of global conformational changes in NTnC during Ca^{2+} titration, and a more complete picture of the Ca^{2+}-induced structural transition was obtained. Third, monitoring structural transitions by NMR techniques as described herein avoids the uncertainties associated with the introduction of large spectral probes by chemical modification or the substitution of naturally occurring amino acids by site-specific mutation. Both approaches may lead to changes in the structure and functional properties of the protein. The perturbation of Ca^{2+} binding properties and the structure of NTnC caused by Phe29 to Trp mutation is demonstrated in the present work and is discussed below. Compared with the spectral probe approach, NMR has the advantage in that every atom in the molecule is potentially a sensitive indicator for the conformational changes in its environment.

In the present NMR study, Ca^{2+} titration of the N-domain was monitored by two-dimensional (2D) {^{1}H, ^{15}N}-HMQC spectral changes. Although the resonances monitored as a function of Ca^{2+} binding occurred at slow, intermediate, and fast exchange rates on the NMR time scale, most of these fell into the fast exchange mode. This permitted chemical shift changes to be followed throughout the Ca^{2+} titration. It was observed that these occurred along the entire amino acid sequence of the N-domain during the binding of both the first equivalent of Ca^{2+} as well as the second. Thus, binding of each equivalent of Ca^{2+} led to structural alterations throughout the N-domain's global structure. The data were best-fitted to a noncooperative model with one binding site 8−10-fold stronger than the other. The determined macroscopic dissociation constants were $0.69\ \mu M \leq K_{D1} \leq 2.65\ \mu M$ for the first Ca^{2+} binding site and $5.8\ \mu M \leq K_{D2} \leq 26\ \mu M$ for the second. These lie in the approximate range of values reported for the low-affinity sites of TnC in the literature [see reviews by Leavis and Gergely (1984) and Graberak et al. (1992); see also Fujimori et al. (1990), da

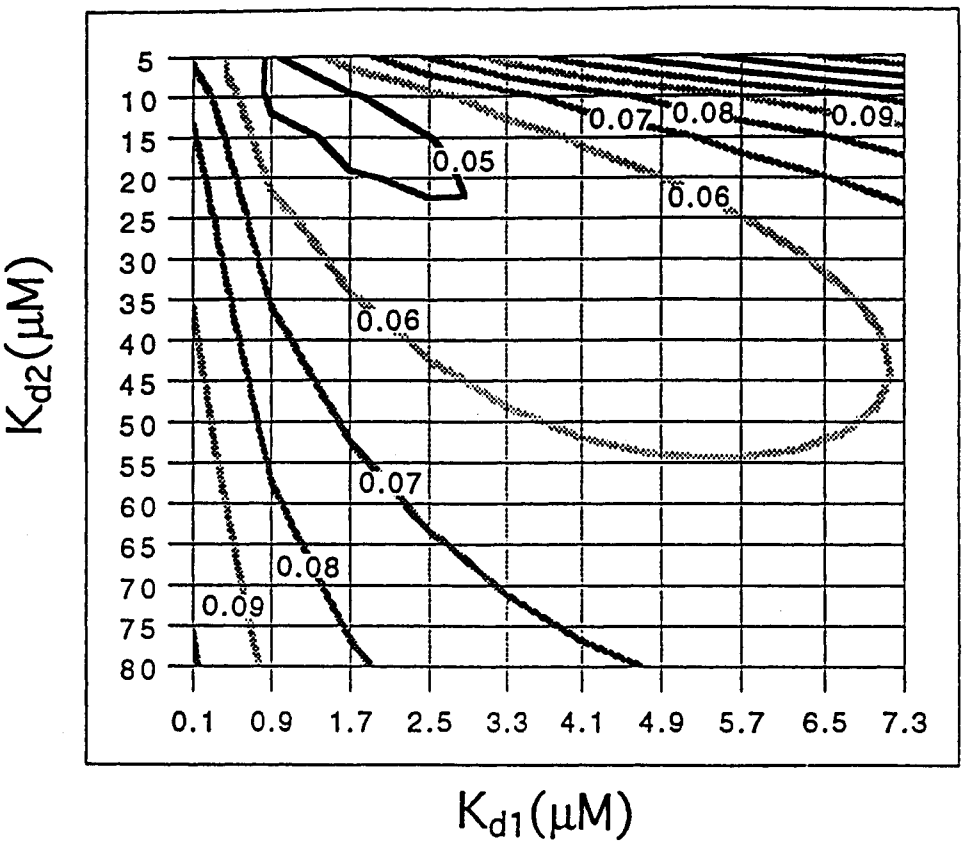

FIGURE 6: Contour plots (fitting of Figure 4B) showing the fit between calculated Ca^{2+} binding curves and the experimental titration data obtained by monitoring the $\{^1H,^{15}N\}$-HMQC spectral changes of 1.5 mM uniformly ^{15}N-labeled NTnC. Fittings of Figures 4A–F all result in similar contours. The fitting procedure was as described under Results. The χ value contours represent the level of agreement between the calculated curves and the titration data.

Silva et al. (1993), Golosinska et al. (1991), Pearlstone et al. (1992a), Li et al. (1994), and Chandra et al. (1994)].

The present analysis indicates that while binding of Ca^{2+} to sites II and I is sequential and in each case leads to structural changes throughout the N-domain, these changes do not affect the Ca^{2+} affinity of the lower affinity site, i.e., absence of cooperativity. The observation that with each Ca^{2+} bound the induced structural changes are global is not surprising in light of the close structural coupling of sites I/II in the crystal structure (Strynadka & James, 1989) and as demonstrated in the melting profiles of the N-domain structure (Tsalkova & Privalov, 1985). In the case of sites III/IV, Shaw et al. (1991, 1992) have shown that the binding of a single Ca^{2+} facilitates the interaction and folding of two polypeptides representing either two Ca^{2+} binding sites III or the two sites III and IV. The present results with intact N-domain are analogous in that the binding of a single Ca^{2+} leads to changes throughout the N-domain structure which apparently account for 80% of the total ellipticity change induced by the binding of $2Ca^{2+}$ (see Figure 8).

The present data do not permit the direct assignment of the N-domain lower and higher affinity sites to structural sites I and/or II, respectively. However, it is tempting to speculate that site II is the stronger of the two based on the amino acids occupying the liganding positions in the two sites. In the coordination geometry of the helix–loop–helix Ca^{2+} binding proteins, the seven liganding positions are arranged as a pentagonal bipyramid [see Strynadka and James (1989)]. The six amino acid residues contributing to these liganding groups are designated in the sequences as positions 1, 3, 5, 7, 9, and 12 (or X, Y, Z, −Y, −X, and −Z, respectively). Although determination of the tertiary structure of the Ca^{2+}-loaded state of NTnC is still in progress (Gagné et al., in preparation), the roles of the amino acid residues occupying these liganding positions in several Ca^{2+} binding proteins have been described (Strynadka & James, 1989). In TnC, positions 1, 3, and 12 are identical in sites I and II. Positions 7 and 9, although occupied by different amino acids in each of the two sites, probably involve ligand formation with main-chain carbonyl oxygens (position 7) or through a H_2O molecule (position 9). The major difference is in position 5 (or Z) in which Ser of site II is replaced by Gly in site I. Examination of the X-ray structures of several Ca^{2+} binding loops shows that the side chain of Ser at this position interacts directly with Ca^{2+} through its O^{γ} atom [see Strynadka and James (1989)]. Its replacement by Gly would be expected to reduce the Ca^{2+} affinity of site I relative to site II (Marsden et al., 1990).

The present NMR data, indicating a substantial difference in the Ca^{2+} affinity of sites I/II and minimal cooperativity in Ca^{2+} binding to those sites, are in contrast to our previous studies in which Ca^{2+} titrations of the fluorescence and far-UV CD of mutants F29W NTnC and intact F29W indicated cooperative Ca^{2+} binding to sites I/II and no detectable differences in their affinities. To rationalize these observations, a direct comparison of the Ca^{2+} titration of the far-UV CD of wild-type NTnC and F29W NTnC was made (see Figure 8). In agreement with our previous observations, the titration curve for the F→W mutant was monophasic. That for the wild-type N-domain was biphasic, from which apparent macroscopic Ca^{2+} dissociation constants could be calculated in reasonable agreement with those derived from

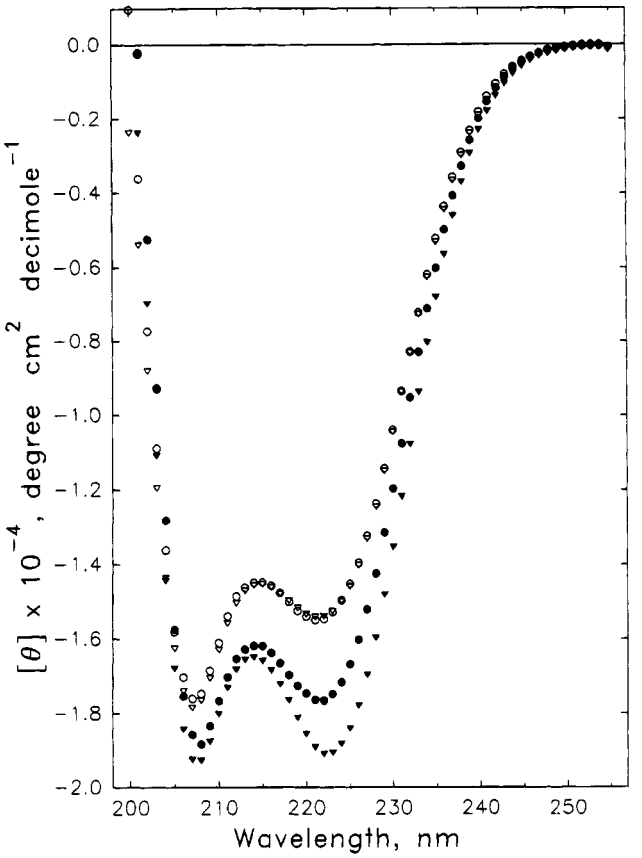

FIGURE 7: Averaged far-UV CD spectra of F29W/NTnC: $-Ca^{2+}$ (▽), $+Ca^{2+}$ (▼); and NTnC: $-Ca^{2+}$ (○), $+Ca^{2+}$ (●). Buffer conditions were 50 mM 3-(*N*-morpholino)propanesulfonic acid, pH 7.1, 100 mM KCl, and 1 mM EGTA, 25 °C; protein concentrations were 30 μM; $-Ca^{2+}$: no $CaCl_2$ added; $+Ca^{2+}$: pCa = 3.

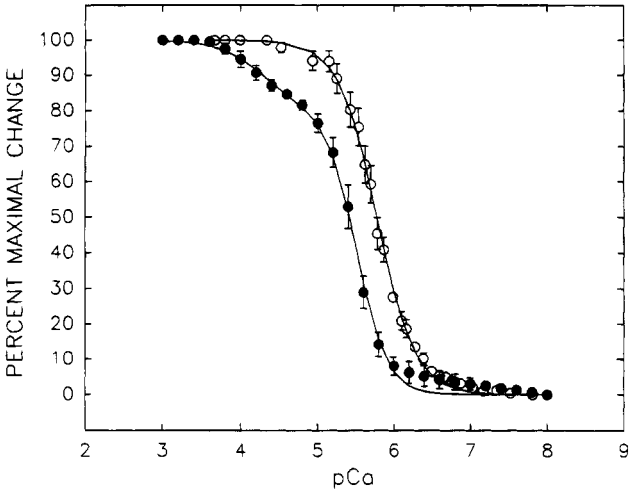

FIGURE 8: Ca^{2+} titration of far-UV CD $[\theta]_{221nm}$ of F29W/NTnC (○) (Li et al., 1994) and NTnC (●). Experimental conditions and protein concentrations were as in Figure 7. Data points are averages of three or more titrations with standard deviations shown as vertical bars. The fitted curves to the averaged data points are shown by solid lines. In the case of NTnC, 80% and 20% of the total $[\theta]_{221nm}$ change were assigned to the higher and lower affinity phases of the biphasic curve, respectively.

the NMR study. We conclude that the substitution of F29 by W has perturbed the Ca^{2+} binding properties of the N-domain. Further evidence comes from comparison of the far-UV CD spectra of the two domains (see Figure 7). In the absence of Ca^{2+}, these spectra are virtually superimposable; in the Ca^{2+}-loaded state, F29W NTnC has significantly increased negative ellipticity particularly in the region of 221 nm when compared with wild-type NTnC. These observations indicating perturbations of both the Ca^{2+} binding properties and structure of the Ca^{2+}-loaded N-domain by the F29 to W substitution are consistent with our recent demonstration that this mutation is deleterious in several functional assays (Chandra et al., 1994).

Differences in Ca^{2+} affinity of the two lower affinity sites from avian or mammalian TnCs have not previously been reported although microcalorimetric studies have indicated such a difference in the case of bull-frog TnC (*Rana catesbeiana*) (Imaizuma et al., 1987, 1990; Imaizuma & Tanokura, 1990). It was found that the edible frog TnC has >90% sequence identity to the protein used in this work (residues 1−90) using the SEQSEE program (Wishart et al., 1994). When spectroscopic techniques were employed to study Ca^{2+} binding to intact TnC, there was always present the large background of Ca^{2+}-induced changes attributable to the C-domain. As shown in our earlier work (Li et al., 1994), only 27% of the total Ca^{2+}-induced ellipticity change in intact TnC is attributable to Ca^{2+} binding to the lower affinity sites located in the N-domain. As a result, only a small portion of the Ca^{2+} titration curve arises from Ca^{2+} binding to the N-domain, which may be inadequate to distinguish two different binding sites. In the case of direct binding studies by equilibrium dialysis, Potter and Gergely (1975) reported for intact rabbit skeletal TnC the presence of two classes of sites, two high-affinity and two lower affinity sites with no apparent cooperativity between sites. Since the Ca^{2+} binding curves for isolated TnC in the absence of the other troponin components were not presented in this study, the question of different Ca^{2+} binding affinities for N-domain sites I/II cannot be critically assessed from their data. Ca^{2+} binding to rabbit skeletal muscle TnC has also been measured using a Ca^{2+} ion sensitive electrode (Iida, 1988), and it was observed that the two higher affinity sites bind Ca^{2+} with positive cooperativity, but the two lower affinity sites bind Ca^{2+} ions independently. That no affinity differences were observed for the N-domain from these studies is not because of the nonexistence of this stepwise binding nature for sites I/II, but because the two binding constants are separated by only a factor of 10 which is not large enough to give rise to a resolved plot (Weber, 1992), especially when a lesser density of data points is encountered, which is often the case in direct binding studies (Potter & Gergely, 1975; Iida, 1988; Fujimori et al., 1990; de Silva et al., 1993). The biphasic feature of the ellipticity change versus pCa observed for the wild-type N-domain in the present work (see Figure 8) is due to the steep slope of the curve associated with the filling of the N-domain's higher affinity site. The physical basis for this steepness is presently unclear although studies have shown that the steepness of a pCa curve can be dependent on the experimental conditions such as temperature, pH, and ionic strength (Rosenfeld &Taylor, 1985). Interestingly, Cheung and co-workers (M. She, P. K. Umeda, and H. C. Cheung, personal communication) have recently shown that Ca^{2+} titration of the fluorescence of a F22W mutant of intact chicken skeletal muscle TnC displays a biphasic curve attributable to the filling of sites I/II, an observation in excellent agreement with the results presented herein. In this case too, the steepness of that portion of the titration curve due to Ca^{2+} binding to the higher affinity site of the N-domain was excessive. Because of the low protein concentrations (2 μM) employed in these

studies, it seems unlikely that this steepness can arise from protein aggregation.

ACKNOWLEDGMENT

We are indebted to Mr. Kim Oikawa for the far-UV CD measurements, Mr. Robert Boyko for his assistance with the curve-fitting program, Mr. Pierre Dubord for amino acid analyses, and Mr. Gerry McQuaid for upkeep of the NMR spectrometer. We thank Mr. Mingda She in Dr. Herbert C. Cheung's laboratory at the University of Alabama at Birmingham for sending us their unpublished data.

REFERENCES

Bax, A., Griffey, R. H., & Hawkins, B. L. (1983) *J. Magn. Reson. 55*, 301−315.
Brzeska, H., Venyaminov, S. V., Grabarek, Z., & Drabikowski, W. (1983) *FEBS Lett. 153*, 169−173.
Campbell, A. P., Cachia, P. J., &Sykes, B. D. (1991) *Biochem. Cell. Biol.* 69, 674−681.
Chandra, M., Fidalgo da Silva, E., Sorenson, M. M., Ferro, J. A., Pearlstone, J. R., Nash, B. E., Borgford, T., Kay, C. M., & Smillie, L. B. (1994) *J. Biol. Chem. 269*, 14988−14994.
da Silva, A. C. R., de Araujo, A. H. B., Herzberg, O., Moult, J., Sorenson, M., & Reinach, F. C. (1993) *Eur. J. Biochem. 213*, 599−604.
Drabikowski, W., Dalgarno, D. C., Levine, B. C., Gergely, J., Grabarek, Z., & Leavis, P. C. (1985) *Eur. J. Biochem. 151*, 17−28.
Drakenberg, T., Forsen, S., Thulin, E., & Vogel, H. J. (1987) *J. Biol. Chem. 262*, 672−678.
Ellis, P. D., Marchetti, P. S., Strang, P., & Potter, J. D. (1988) *J. Biol. Chem. 263*, 10284−10288.
Evans, J. S., Levine, B. A., Leavis, P. C., Gergely, J., Grabarek, Z., & Drabikowski, W. (1980) *Biochem. Biophys. Acta 623*, 10−20.
Findlay, W. A., & Sykes, B. D. (1993) *Biochemistry 32*, 3461−3467.
Findlay, W. A., Sönnichsen, F. D., & Sykes, B. D. (1994) *J. Biol. Chem. 269*, 6773−6778.
Fujimori, K., Sorenson, M., Herzberg, O., Moult, J., & Reinach, F. C. (1990) *Nature 345*, 182−184.
Gagné, S. M., Tsuda, S., Li, M. X., Chandra, M., Smillie, L. B., & Sykes, B. D. (1994) *Protein Sci. 3*, 1961−1974.
Golosinska, K., Pearlstone, J. R., Borgford, T., Oikawa, K., Kay, C. M., Carpenter, M. R., & Smillie, L. B. (1991) *J. Biol. Chem. 266*, 15797−15809.
Grabarek, Z., Grabarek, J., Leavis, P. C., & Gergely, J. (1983) *J. Biol. Chem. 258*, 14098−14102.
Grabarek, Z., Tan, R.-Y., Wang, J., Tao, T., & Gergely, J. (1990) *Nature 345*, 132−135.
Grabarek, Z., Tao, T., & Gergely, J. (1992) *J. Muscle Res. Cell Motil. 13*, 383−393.
Griffiths, P. J., Potter, J. D., Coles, B., Strang, P., & Ashley, C. C. (1984) *FEBS Lett. 176*, 144−150.
Güth, K., & Potter, J. D. (1987) *J. Biol. Chem. 262*, 13627−13635.
Herzberg, O., & James, M. N. G. (1988) *J. Mol. Biol. 203*, 761−768.
Herzberg, O., Moult, J., & James, M. N. G. (1986) *J. Biol. Chem. 261*, 2638−2644.
Hincke, M. T., McCubbin, W. D., & Kay, C. M. (1978) *Can. J. Biochem. 56*, 384−395.
Iida, S. (1988) *J. Biochem. (Tokyo) 103*, 482−486.
Ikura, M., Clore, G. M., Cronenborn, A. M., Zhu, G., Klee, C. B., & Bax, A. (1992) *Science 256*, 632−638.
Imaizumi, M., & Tanakura, M. (1990) *Eur. J. Biochem. 192*, 275−281.
Imaizumi, M., Tanakura, M., & Yamada, K. (1987) *J. Biol. Chem. 262*, 7963−7966.
Imaizumi, M., Tanakura, M., & Yamada, K. (1990) *J. Biochem. 107*, 127−132.
Johnson, J. D., Collins, J. H., & Potter, J. D. (1978) *J. Biol. Chem. 253*, 6451−6458.
Johnson, J. D., Charlton, S. C., & Potter, J. D. (1979) *J. Biol. Chem. 254*, 3497−3502.
Krudy, G. A., Brito, R. M. M., Putkey, J. A., & Rosevear, P. R. (1992) *Biochemistry 31*, 1595−1602.
Leavis, P. C., & Gergely, J. (1984) *CRC Crit. Rev. Biochem. 16*, 235−305.
Leavis, P. C., Rosenfeld, S. S., Gergely, J., Grabarek, Z., & Drabikowski, W. (1978) *J. Biol. Chem. 253*, 5452−5457.
Leavis, P. C., Nagy, B., Lehrer, S. S., Bialkowsky, H., & Gergely, J. (1980) *Arch. Biochem. Biophys. 200*, 17−21.
Levine, B. A., Mercola, D., Coffman, D., & Thornton, J. M. (1977) *J. Mol. Biol. 115*, 743−760.
Li, M. X., Chandra, M., Pearlstone, J. R., Racher, K. I., Trigo-Gonzalez, G., Borgford, T., Kay, C. M., & Smillie, L. B. (1994) *Biochemistry 33*, 917−925.
Marsden, B. J., Shaw, G. S., & Sykes, B. D. (1990) *Biochem. Cell Biol. 68*, 587−601.
Pearlstone, J. R., Borgford, T., Chandra, M., Oikawa, K., Kay, C. M., Herzberg, O., Moult, J., Herklotz, A., Reinach, F. C., & Smillie, L. B. (1992a) *Biochemistry 31*, 6545−6553.
Pearlstone, J. R., McCubbin, W. D., Kay, C. M., Sykes, B. D., & Smillie, L. B. (1992b) *Biochemistry 31*, 9703−9708.
Potter, J. D., & Gergely, J. (1975) *J. Biol. Chem. 250*, 4628−4633.
Potter, J. D., & Johnson, J. D. (1982) in *Calcium and Cell Function* (Cheung, W., Ed.) Vol. 2, pp 145−173, Academic Press, New York.
Potter, J. D., Charlton, S. C., & Johnson, J. D. (1981) *Fed. Proc., Fed. Am. Soc. Exp. Biol. 40*, 2653−2656.
Rosenfeld, S. S., & Taylor, E. W. (1985) *J. Biol. Chem. 260*, 242−251.
Satyshur, K. A., Rao, S. T., Pyzalska, D., Drendel, W., Greaser, M., & Sundaralingam, M. (1988) *J. Biol. Chem. 263*, 1628−1647.
Seamon, K. B., Hartshorne, D. J., & Bothner-By, A. A. (1977) *Biochemistry 16*, 4039−4046.
Shaka, A. J., Keeler, J., Frenkiel, T., & Freeman, R. (1983) *J. Magn. Reson. 52*, 335−338.
Shaw, G. S., Golden, L. F., Hodges, R. S., & Sykes, B. D. (1991) *J. Am. Chem. Soc. 113*, 5557−5563.
Shaw, G. S., Hodges, R. S., & Sykes, B. D. (1992) *Biopolymers 32*, 391−397.
Strynadka, N. C. J., & James, M. N. G. (1989) *Annu. Rev. Biochem. 58*, 951−998.
Tsalkova, T. N., & Privalov, P. L. (1985) *J. Mol. Biol. 181*, 533−544.
Tsuda, S., Hasegawa, Y., Yoshida, M., Yagi, K., & Hikichi, K. (1988) *Biochemistry 27*, 4120−4126.
Tsuda, S., Ogura, K., Hasegawa, Y., Yagi, K., & Hikichi, K. (1990) *Biochemistry 29*, 4951−4958.
Weber, G. (1992) in *Protein Interactions*, pp 45−46, Chapman and Hall, New York.
Williams, T. C., Shelling, J. G., & Sykes, B. D. (1985) in *NATO Advanced Study Institution on NMR in the life sciences* (Bradbury, E. M., & Nicolini, C., Eds.) 93−103, Plenum Press, New York.
Williams, T. C., Corson, D. C., & Sykes, B. D. (1987) *J. Biol. Chem. 262*, 6248−6256.
Wishart, D. S., Boyko, R. F., Willard, L., Richards, F. M., & Sykes, B. D. (1994) *Comput. Appl. Biosci. 10*, 121−132.
Zot, A. S., & Potter, J. D. (1987a) *J. Biol. Chem. 262*, 1966−1969.
Zot, H. G., & Potter, J. D. (1987b) *J. Muscle Res. Cell Motil. 8*, 428−436.
Zot, A. S., & Potter, J. D. (1987c) *Annu. Rev. Biophys. Biophys. Chem. 16*, 535−559.
Zot, A. S., & Potter, J. D. (1989) *Biochemistry 28*, 6751−6756.
Zot, H. G., Güth, K., & Potter, J. D. (1986) *J. Biol. Chem. 261*, 15883−15890.

BI9429243